An intermetamorphic larval stage of a mantis shrimp and its contribution to the 'missing-element problem' of stomatopod raptorial appendages

Abstract

In eumalacostracan crustaceans the thoracic appendages usually have seven elements along the main axis of the appendage. Mantis shrimps are an exception: their raptorial sub-chelate maxillipeds (anterior thoracopods) have only six such elements. Hence it has been speculated which two of the original seven elements have become conjoined in mantis shrimps. So far this question remains unanswered due to the lack of a proper reference point of identifying individual original elements. One candidate for such a reference point would be the exopod, which is unfortunately absent in adult stomatopods. Antizoea larvae possess exopods on the maxillipeds, but lack subdivision along the main axis of the appendage. We describe here a specimen that is right in the transition between the antizoea larval phase and the next larval phase (erichthus). It still possesses an exopod, but also additionally a subdivision into discrete elements on the maxillipeds. With this it provides an important reference scheme for solving the elemental identity in mantis shrimp maxillipeds. It clearly falsifies the suggestion that the basipod has become either conjoined with the coxa or endopod element 1 (ischium). In combination with data from the fossil record we suggest that stomatopods possess a carpo-propodus.

Key words: Stomatopoda; larva; antizoea; palaeo-evo-devo; metamorphosis

Introduction

Eumalacostracan crustaceans include all the forms that most people will easily recognise as a crustacean, for example shrimps, prawns, crabs, wood lice, krill and all their closer relatives. Eumalacostraca is characterised by a number of autapomorphies. Among these is a distinct tagmosis, or body organisation. The body of most eumalacostracans includes 20 segments: six segments form the head, eight segments the thorax (thorax I of Walossek & Müller 1998) and six segments the pleon (often imprecisely termed “abdomen”). The thorax segments usually bear the most prominent appendages. These thorax appendages, or thoracopods, consist in the eumalacostracan ground pattern (the morphology of the “reconstructed ancestor”) of seven elements along the (seeming) main axis (see e.g. Wolff & Scholtz 2008 for axis discussion). These are: the proximal coxa, the basipod (also basis), which in many forms bears latero-distally the exopod (“swimming branch”), and medio-distally the endopod with five more elements called ischium, merus, carpus, propodus and dactylus (from proximally to distally; see Fig. 1A). This morphology and the names have sometimes been erroneously projected into the eucrustacean ground pattern, but in this strict form it only accounts for Eumalacostraca (e.g. Waloszek 2003; Schram 2007).

Yet, this does not mean that there are no notable exceptions from the general pattern of seven elements in the thoracopods. One example is Stomatopoda, or at least for sure its ingroup with all modern representatives, Verunipeltata. The representatives of Verunipeltata, modern mantis

shrimps, have two distinct sets of thoracopods: the anterior five pairs are sub-chelate and mainly used for grasping (see e.g. Haug C. et al. 2012); they are also called maxillipeds. The posterior three pairs of thoracopods are mainly used for walking.

The maxillipeds are sub-similar, but further differentiated. They represent a cleaning appendage (1st maxilliped), the major raptorial appendage or ballistic claw (2nd maxilliped) and three pairs of smaller claws (3rd-5th maxilliped; e.g. Haug C. et al. 2012). These appendages will be treated in more detail in the following.

All these appendages have six elements along their main axis and lack an exopod. As there are only six elements present, one element appears to be missing in comparison to the eumalacostracan ground pattern. As Schram (2007) has reviewed, there are different interpretations for this phenomenon. Most interpretations seem to agree that two of the original seven elements become fused or better, without implying a process, are now conjoined (as 'fusion' implies a process in which two separate entities become one, while also no division may have occurred). Yet, there are different interpretations which of the two elements are conjoined, for example: ischium and merus = ischio-merus (Hothuis & Manning 1969; McLaughlin 1980; Schram 1986; Westheide & Rieger 2007); basipod and ischium = basi-ischium (Gruner 1993); coxa and basipod = coxo-basis (Ahyong pers. com. in Schram 2007; summarised in Fig. 1B-D).

Schram (2007) nicely pointed out that this confusion is mainly caused by the lack of an important reference point: the exopod. If an exopod would be present, its proximal articulation would clearly identify the latero-distal region of the basipod (Fig. 1E-G). Yet, as stated above, the mantis shrimp maxillipeds lack an exopod.

And, as before, there is in fact an exception: There are specific larval stages of certain mantis shrimps that have an exopod on the maxillipeds. Mantis shrimp larval development is a comparably understudied field (see Ahyong et al. 2014 for a recent review; Haug & Haug 2014, Haug C. et al. 2015 for new finds). Generally there are two types of early larval forms within Stomatopoda: the pseudozoea and the antizoea.

The pseudozoea has the anterior two maxillipeds already developed and these roughly resemble the adult condition; further posterior thoracic appendages develop stepwise. Swimming is performed by (some of) the already developed pleopods.

The antizoea has five pairs of thoracopods which are biramous, hence possessing the exopod, which are used for swimming. Unfortunately, in these forms the endopod does not show marked subdivision as does in fact the entire appendage (Ahyong et al. 2014). Still, finding a very late antizoea which already shows some of the future subdivision of the sub-chelate appendages could provide the important marker point that Schram (2007) has suggested: the insertion of the exopod.

We present here the detailed description of such a larva that is just in the process of transforming from an antizoea into a later, so-called erichthus stage. We discuss the implications of the observed morphology on the 'missing-element problem' of stomatopod raptorial appendages.

Material and Methods

Material

One specimen central to this study comes from the collection of the Zoological Museum of the University of Copenhagen (ZMUC 3723_V_E; in the following specimen A). It was collected during the famous Dana expedition (see also Haug & Haug 2014). A specimen for comparison, representing a “true” antizoea comes from the same collection (ZMUC 3567_II_F; in the following specimen B). Final museum numbers will be added later

Preparation

For documentation specimens were fixed with cover slips within their original storage liquid. The comparative specimen (Specimen B) was dissected after initial documentation in 70% ethanol under

an Olympus SZX7 dissection microscope using zoological preparation tools. Isolated parts were then placed in small glass trays with 70% ethanol and fixed with cover clips or small metal nuts for documentation. For further storage all appendages and remaining structures were stored in separate Eppendorf-type cups with screw lids.

Documentation methods

1) Specimen A was initially documented by macrophotography (Fig. 2A, B). A Canon Rebel T3i equipped with a macro lens (MP-E 65mm) equipped with a polarization filter was used. Illumination was provided by a Macro Twin Lite (MT24EX) flash. In order to produce cross-polarized light perpendicular polarization filters were placed on the flashes. This increases the color contrast and reduces reflections (e.g. Hörnig et al. 2014: fig. 2). Several images (frames) in different focal planes were recorded (also called a stack; e.g. Haug J.T. et al., 2008; 2011; Haug C. et al., 2009).
2) Specimen B was initially documented on a compound microscope with a 10x lens resulting in about 100x magnification (Fig. 2C). Transmitted light was used for illumination. Several image details had to be recorded due to the size of the specimen. Each image detail was documented with a stack of images (composite imaging Haug J.T. et al., 2008; 2011; Haug C. et al., 2009)
3) Specimen A was further documented in 70% ethanol on a Keyence BZ-9000 epi-fluorescence microscope with a 4x and 10x objective (resulting in about 40x and 100x magnification; Figs. 3-5). UV light (377 nm) was used for illumination (e.g Haug C. et al., 2009) exploiting the auto-fluorescence capacities of the specimen. Also here several image details were documented, each with a stack of images.
4) Specimen B was further documented on a Leica SP TCS confocal laser scanning microscope (cLSM) with a 10x objective (Fig. 6-8). Blue light (488nm) was used as an excitation wavelength. Several image details were recorded, each with a stack.
5) After dissection, individual structures of specimen B were further documented in 70% ethanol on a Keyence BZ-9000 epi-fluorescence microscope with a 10x and 20x objective (resulting in about 100x and 200x magnification; Figs. 7-9). Further settings as described above under 3). Image details with weakly fluorescent structures were recorded a second time with longer exposure time. Some structures were additionally documented under bright field settings (Fig. 7B) or phase contrast settings (Fig. 7C).

Data processing

1) Image stacks for each image detail documented with macro settings, transmitted light or epi-fluorescence were fused with CombineZM/ZP into consistently sharp images.
2) Image stacks for each image detail documented with cLSM were Z-projected (maximum intensity) in FIJI, resulting in consistently sharp images.
3) Resulting sharp images were stitched to panorama images either with Adobe Photoshop CS3 or 4, Adobe Photoshop Elements 11 or Microsoft Image Composite Editor.
4) For adding information from overexposed images (see documentation methods 5) the image was placed in Adobe Photoshop as a separate layer above the image with shorter exposure time. The magic wand tool was applied to mark overexposed areas; a feather with a high radius was applied to the edge, then these overexposed areas were removed. The resulting image shows all parts well illuminated (see Haug C. et al., 2013). Similarly in some images information was added from the bright field images (e.g. setules). Images were desaturated, inverted and treated as overexposed images.
5) Resulting images were finally edited in Adobe Photoshop CS 1, 2 or 3 (optimization of the histogram and sharpness, manual removing of dirt particles and background etc.).
6) For identifying structures on overview images these were marked using a lasso tool and colorized with the colour balance tool, preserving the original shading.
7) Schematic drawings were produced in Adobe Illustrator CS2 (Figs. 1, 10).
8) For comparisons 3D-models of fossil mantis shrimps are presented (Fig. 11; models from Haug

J.T. et al. 2010).

Description
The morphological description is provided as a descriptive matrix (Haug J.T. et al. 2012). Matrix is based on earlier work by Wiethase et al. (in review).

Results

Description of specimen A

Body organised in 20 segments, 1 ocular segment followed by 19 segments. Dorsal organisation of body difficult to assess, due to small size and lack of clear border of structures (Fig. 2A; 3A).

Anterior segments apparently dorsally forming large shield. Exact identity of contributing segments unclear.

Shield large, prominent (Fig. 2A, B); covering most of the body, only very posterior segments and telson protruding from underneath it. In dorsal view roughly rounded pentagonal. Anteriorly tapering into distinct spine (rostrum); from anterior gently widening; widest dimension at about half the anterior-posterior axis; further posteriorly slightly narrower again; curving gently inwards; posterior rim straight; latero-posterior corners with distinct pockets (=doublure on ventral side); latero-posterior corners drawn out into distinct spines. Rostrum long; more than 50% of the length of the shield. Latero-posterior spines long; more than 30% of the length of the shield.

Post-ocular segments 14-18 (pleon segments 1-5) with separate dorsal sclerotisations (tergites).

Post-ocular segment 19 (pleon segment 6) not yet set off from telson.

Telson more or less trapezoid in outline (in ventral view); with three spines on each lateral rim; posterior rim curly-brace-shaped, with one spine as extension of the lateral rim on each side, and 18 spines on the posterior rim of the telson; gaps between spines equipped with small spines.

Ocular segment ventrally bearing stalked compound eyes (Fig. 3). Compound eye differentiable into two parts; proximal stalk and distal ommatidia-bearing region. Appendage derivative of ocular segment, hypostome-labrum complex, well developed. Labrum triangular to heart-shaped in ventral view (Fig. 3D, E).

Appendage of 1st post-ocular segment (antennula, Fig. 3B, C) with 2 peduncle elements and 2 rudimentary flagella distally. Peduncle element 1 (proximal element) tube-shaped; about 1.8x as long as wide. Peduncle element 2 (distal element) tube-shaped but widening distally; about 1.7x as long as peduncle element 1. Flagellum 1 cone-shaped, tapering distally, without any subdivision; shorter than peduncle element 2; distally with at least 3 elongate setae. Flagellum 2 cone-shaped, tapering distally, without any subdivision; longer than flagellum 1; longer then peduncle element 2; distally with at least 1 elongate seta.

Appendage of 2nd post-ocular segment (antenna; Fig. 3B, C) composed of 2 elements. Proximal element (coxa?; protopod?) tube-shaped; about 1.5x as long as wide. Distal element (endopod+basipod?; endopod?) tube-shaped, with a rounded tip; about 4x as long as wide; about 3x as long as proximal elements; 4 setae on tip of distal element.

Appendage of 3rd post-ocular segment (mandible; Fig. 3D, E) without apparent palp; lateral-median dimensions about 2.7x as long as anterior-posterior dimension; further details concealed by labrum. Sternal protrusion of mandibular segment (paragnaths; Fig. 3D, E) as a pair of distinct lobes; posteriorly restricting the movement of the mandibles.

Appendage of 4th post-ocular segment (maxillula; Fig. 3D, E) differentiated into coxa with coxal endite, basipod with basipodal endite and endopod. Coxa more or less triangular (in posterior view; without endite); about 1.2x as long (proximo-distally) as maximum width (medio-laterally); bearing lobe-like endite on the distal part of the medial margin. Coxal endite with a prominent spine

proximally, at least 4 smaller spines further distally. Basipod subtriangular (in posterior view; without endite). Basipodal endite lobe-like with about 5 spines on the median margin. Endopod small, spine-like.

Appendage of 5th post-ocular segment (maxilla; Fig. 3D, E) substructures not yet discernible; more or less tube-shaped; about 3x as long as wide.

Appendage of 6th post-ocular segment (maxilliped 1; Fig. 5A-C) with coxa and basipod carrying endopod and exopod. Coxa more or less tube-shaped (slightly compressed in anterior-posterior axis), about 1.7x as long as wide. Basipod tube-shaped (slightly compressed in anterior-posterior axis); about 2x as long as wide; bearing endopod and exopod. Endopod divided into proximal and distal part; proximally not yet subdivided, future subdivision into elements indicated by faint lines; distal element set off from proximal part, about 1.1x as long as wide (in posterior view); with 2 setae on distal tip. Exopod elongate paddle-shaped, with a rounded tip; about 7.5x as long as wide.

Appendage of 7th post-ocular segment (maxilliped 2; Fig. 4) with 6 main elements; coxa, basipod with endopod with 4 elements and exopod; endopod element 3 and 4 forming a subchela. Coxa more or less tube-shaped (slightly compressed in anterior-posterior axis); dimensions difficult to assess; longer than wide. Basipod more or less tube-shaped (slightly compressed in anterior-posterior axis); about as long as wide; width similar to coxa. Endopod element 1 elongate; about as wide as basipod, but 2x as long. Endopod element 2 short; as wide as basipod, but only about 50% of its length. Endopod element 3 massive; broader than preceding elements; slightly shorter than element 2. Endopod element 4 elongate spine/blade-like; only slightly shorter than element 3, but significantly more slender; proximally curved. Exopod comparably small; elongate paddle-shaped, smaller than endopod element 2; distally with 3 indentations indicating seta insertions.

Appendage of 8th post-ocular segment (maxilliped 3; Fig. 5A-C) with coxa and basipod carrying endopod and exopod. Coxa more or less tube-shaped (slightly compressed in anterior-posterior axis); dimensions difficult to assess. Basipod tube-shaped (slightly compressed in anterior-posterior axis); about 1.7x as long as wide. Endopod tapering distally with a rounded tip; about 3.5x as long as wide; about 1.8x as long and about 0.8x as wide as basipod; with indications (indentations) of setae towards the distal end. Exopod elongate paddle-shaped with a rounded tip; about 4.3x as long as wide; with setae on inner and outer lateral rim and on the tip of exopod indicated by indentations.

Appendage of 9th post-ocular segment (maxilliped 4; Fig. 5A-C) with coxa and basipod carrying endopod and exopod. Coxa not accessible. Basipod not accessible. Endopod not accessible. Exopod with rounded tip and setae.

Appendage of 10th post-ocular segment (maxilliped 5; Fig. 5A-C) with coxa and basipod carrying endopod and exopod. Coxa not accessible. Basipod not accessible. Endopod roughly tube-shaped. Exopod elongate paddle-shaped; with serrations on the tip as indications for setae.

Appendages of 11th-13th post-ocular segments (thoracopod 6-8) apparently not yet developed.

Appendage of 14th post-ocular segment (pleopod 1; Fig. 5A, D, E) with basipod carrying endopod and exopod. Basipod difficult to measure; roughly rectangular (in anterior view) slightly wider than long. Endopod paddle-shaped; with one prominent spine as extension of the median edge, pointing distally. Exopod paddle-shaped; with serrations on the lateral rim as indication for setae.

Appendage of 15th post-ocular segment (pleopod 2; Fig. 5A, D, E) with basipod carrying endopod and exopod; sub-similar to, but smaller than preceding appendage. Basipod roughly rectangular (in anterior view), slightly widening distally; wider than long. Endopod paddle-shaped; with one prominent spine as extension of the median edge, pointing distally. Exopod paddle-shaped; with serrations on the lateral rim as indication for setae.

Appendage of 16th post-ocular segment (pleopod 3; Fig. 5A, D, E) with basipod carrying endopod and exopod; sub-similar to, but smaller than preceding appendage. Basipod difficult to assess; roughly rectangular, wider than long. Endopod paddle-shaped. Exopod paddle-shaped.

Appendage of 17th post-ocular segment (pleopod 4; Fig. 5A, D, E) with basipod carrying endopod and exopod; sub-similar to, but smaller than preceding appendage. Basipod more or less rectangular (in anterior view). Endopod and exopod not yet fully articulated from basipod; paddle-shaped (in anterior view).

Appendage of 18th post-ocular segment (pleopod 5) not found, most likely not yet developed.

Appendage of 19th post-ocular segment (uropod) not found, most likely not yet developed.

Description of specimen B

Body organised in 20 segments, 1 ocular segment followed by 19 segments (Figs. 2C, 6). Dorsal organisation of body difficult to assess, due to small size and lack of clear border of structures.

Anterior segments apparently dorsally forming large shield. Exact identity of contributing segments unclear.

Shield large, prominent; covering most of the body, only very posterior segments and telson protruding from underneath it. In dorsal view roughly rounded pentagonal. Anteriorly tapering into distinct spine (rostrum); from anterior gently widening; widest dimension at about half the anterior-posterior axis; further posteriorly slightly narrower again; curving gently inwards; posterior rim straight; latero-posterior corners with distinct pockets (=doublure on ventral side); latero-posterior corners drawn out into distinct spines. Rostrum short; about 30% of the length of the shield. Latero-posterior spines short; about 20% of the length of the shield.

Post-ocular segments 14-18 (pleon segments 1-5) with separate dorsal sclerotisations (tergites).

Post-ocular segment 19 (pleon segment 6) not yet set off from telson.

Telson more or less trapezoid in outline (in ventral view); with three spines on each lateral rim; posterior rim curly-brace-shaped; with one spine as extension of the lateral rim on each side, two prominent spines on the tip of the convex part of the posterior rim, and 14 spines on the posterior rim of the telson; gaps between spines equipped with small spines.

Ocular segment ventrally bearing stalked compound eyes (Fig. 7A). Compound eye differentiable into two parts; proximal stalk and distal ommatidia-bearing region. Appendage derivative of ocular segment, hypostome-labrum complex, well developed. Hypostome with distinct spine-like protrusion (frontal horn; Fig. 8A-E). Labrum triangular to heart-shaped in ventral view.

Appendage of 1st post-ocular segment (antennula; Fig. 7A, B) with 2 peduncle elements (proximal element not completely preserved through preparation) and indication of one future flagellum distally. Peduncle element 1 (proximal element) tube-shaped; not completely preserved due to preparation. Peduncle element 2 (distal element) tube-shaped; as long as wide. Single flagellum cone-shaped, tapering distally, without any subdivision; longer than peduncle element 2; distally with at least 1 elongate seta.

Appendage of 2nd post-ocular segment (antenna; Fig. 7A, C) with 3 elements (coxa, basipod and endopod?). Element 1 (coxa?) tube-shaped; about as long as wide. Element 2 (basipod?)tube-shaped; about as wide as preceding element; slightly longer.

Appendage of 3rd post-ocular segment (mandible; Fig. 8A-E) without apparent palp; lateral-median dimensions about 1.5x as long as anterior-posterior dimension. With pronounced but largely undifferentiated gnathal edge. Sternal protrusion of mandibular segment (paragnaths) as a pair of distinct lobes; posteriorly restricting the movement of the mandibles.

Appendage of 4th post-ocular segment (maxillula; Fig. 8A-E) differentiated into coxa with coxal endite and basipod with basipodal endite. Coxa more or less triangular (in posterior view; without endite); about 1.6x as long as maximum width; bearing lobe-like endite on the distal part of the medial margin. Coxal endite with about 5 spines along the median edge. Basipod subtriangular (in posterior view; without endite). Basipodal endite about 1.6x as long as wide; lobe-like with

about 5 spines on the median margin.

Appendage of 5th post-ocular segment (maxilla) not identifiable, most likely not yet developed.

Appendage of 6th post-ocular segment (maxilliped 1; Figs. 6, 9) with coxa and basipod carrying endopod and exopod. Coxa more or less tube-shaped (slightly compressed in anterior-posterior axis), about 1.1x as long as wide. Basipod tube-shaped (slightly compressed in anterior-posterior axis); about 1.2x as long as wide; bearing endopod and exopod. Endopod divided into two elements; about 4.3x as long as wide; element 1 about 4.3x as long as element 2; with 6 setae on distal tip. Exopod elongate paddle-shaped, with a rounded tip; about 5.5x as long as wide; with 4 setae on distal tip of element 2; about 1.45x as long as endopod.

Appendage of 7th post-ocular segment (maxilliped 2; Figs. 6, 9) with 4 main elements; coxa, basipod with exopod and endopod; exopod consisting of two elements. Coxa more or less tube-shaped (slightly compressed in anterior-posterior axis), about 1.1x as long as wide. Basipod tube-shaped (slightly compressed in anterior-posterior axis); about 1.2x as long as wide; bearing endopod and exopod. Endopod broad paddle-like; subdivided into two distinct parts; proximal part about as large as coxa; distal part significantly smaller, with 4 setae distally. Exopod smaller; paddle-shaped, about 3x as long as wide; with at least 6 setae on disto-lateral rim.

Appendage of 8th post-ocular segment (maxilliped 3; Figs. 6, 9) with coxa and basipod carrying endopod and exopod. Coxa more or less tube-shaped (slightly compressed in anterior-posterior axis); about 1.2x as long as maximum width. Basipod tube-shaped (slightly compressed in anterior-posterior axis); about as long as wide; with one seta. Endopod consisting of two elements; about 2.3x as long as maximum width; element 1 is more or less tube-shaped and about 1.5x as long as maximum width with about 4 setae; element 2 is about 0.8x as long as wide with 4 setae on distal tip; element 1 is about 4 times as long as element 2 and about 2x as wide as element 2. Exopod elongate paddle-shaped with a rounded tip; with at least four setae along disto-lateral margin.

Appendage of 9th post-ocular segment (maxilliped 4; Figs. 6, 9) with coxa and basipod carrying endopod and exopod. Coxa more or less tube-shaped (slightly compressed in anterior-posterior axis); about as long as wide. Basipod more or less tube-shaped (slightly compressed in anterior-posterior axis); about 1.4x as long as wide. Endopod more or less tube-shaped to paddle-shaped; about 2.5x as long as wide (in anterior view); consisting of 2 elements; element 1 about 2x as long as wide, with 2 plumose setae on the outer lateral rim; element 2 about as long as wide; with 4 plumose setae on distal tip of element 2. Exopod elongate paddle-shaped; about 3x as long as wide; with 7 plumose setae on distal tip; about 1.2x as long as endopod.

Appendage of 10th post-ocular segment (maxilliped 5; Figs. 6, 9) with coxa and basipod carrying endopod and exopod. Coxa more or less tube-shaped (slightly compressed in anterior-posterior axis); about as long as wide. Basipod more or less tube-shaped (slightly compressed in anterior-posterior axis); about as long as wide. Endopod more or less tube-shaped to paddle-shaped; about 2.3x as long as wide (in anterior view); consisting of 2 elements; element 1 about 1.7x as long as wide, with 2 setae on the outer lateral rim; element 2 about as long as wide; with 3 plumose setae on distal tip of element 2. Exopod elongate paddle-shaped; about 3x as long as wide; with 6 plumose setae on distal tip; about 1.2x as long as endopod.

Appendages of 11th-13th post-ocular segment (thoracopod 6-8) apparently not yet developed.

Appendages of 14th-17th post-ocular segment (pleopod 1-4; Fig. 9) not found (probably not yet developed).

Appendage of 18th post-ocular segment (pleopod 5; Fig. 6) visible under the cuticle; with basipod carrying endopod and exopod; more or less in a primordial condition, without setae. Basipod more or less rectangular (in anterior view). Endopod and exopod paddle-shaped (in anterior view).

Appendage of 19th post-ocular segment (uropod) not found, most likely not yet developed.

Comparison between specimen A and B

Both specimens have a sub-similar overall morphology of the shield. Yet, in specimen A the spines are significantly longer than in specimen B, indicating its advanced developmental state.

Both specimens possess well-developed compound eyes. Those of specimen B appear more spherical, while those of specimen A appear much more elongate; also this is most likely coupled to a more advanced developmental state of specimen A.

The antennula is more differentiated in specimen A. Peduncle elements are already more elongate, and there are already two flagella, while peduncle elements are stouter and there is only one flagellum in specimen B.

The antenna on the other hand is further developed in specimen B. There are three distinct elements with very elongate setae distally. In specimen A the antenna has only two elements and less pronounced setae.

Maxillula and maxilla are again further developed in specimen A. The maxillula of specimen B still lacks the endopod, which is present in specimen A. The maxilla is still very rudimentary in specimen A, but seems to be still entirely absent in specimen B.

In specimen A the second maxilliped is already attaining the sub-chelate claw shape of the adult. In specimen B all maxillipeds are sub-similar swimming appendages.

Pleopods seem already functional in specimen A, at least the anterior four ones. In specimen B there is no external trace of pleopods, but at least one seems visible through the cuticle.

Discussion

Developmental mode in stomatopods via an antizoea

In most stomatopod groups the early larva is of the so-called pseudozoea type. Such larvae swim with, at least some of, the pleopods. Their maxillipeds are not yet necessarily functional, but already foreshadow their later raptorial morphology. Of the 500 extant stomatopod species we know the larval sequences of only a handful (e.g. Gohar & Al-Kholy 1957; Manning & Provenzano 1963; Pyne 1972; Provenzano & Manning 1978; Morgan & Provenzano 1979; Greenwood & Williams 1984; Hamano & Matsuura 1987; Morgan & Goy 1987). All these seem to develop via a pseudozoea.

Hence our knowledge on stomatopods developing via a antizoea is rather limited. It also remains unclear if only lysiosquilloids develop via such a larva or if also erythrosquilloids have such a type of larva (Ahyong et al. 2014). As our knowledge is still so limited the description of the two specimens here is a cruzial amendment. Antizoeae are known to develop into an erichthus-type larva (Ahyong et al. 2014).

Ahyong & Harling (2000) suggested that the antizoea is a derived type of larva based on phylogenetic reconstructions. Yet, based on its morphology it appears much more plesiomorphic than the pseudozoea: 1) It possesses biramous thoracopods, which represents a rather ancestral condition. 2) It appears to develop the appendages in a stricter anterior-posterior gradient than the pseudozoea, which also represents an ancestral feature (e.g. Haug & Haug 2015).

Yet, this does not exclude that the antizoea could be a derived type of larva. It mainly demonstrates that in stomatopods heterochrony (the evolutionary shift in developmental timing) appears to have played a major role (e.g. Haug & Haug 2015). We clearly need more developmental data on stomatopods that develop via an antizoea before we can easily draw further reaching conclusions.

It is unlikely that the two specimens presented here represent two stages of the same species. This can be concluded from the size as well as the subtle sequential differences. While overall specimen A is further developed than specimen B, the antenna of specimen B is already further differentiated (cf. Figs. 3 vs 7). While specimen B is what we would expect from an antizoea, specimen A indeed partly derives from our expectations. Still the two here described specimens

provide interesting details discussed in the following.

Developmental status of specimen A: intermetamorphic

Stomatopods that start out their post-embryonic ontogeny as an antizoea have two major morphological changes in their sequence that can be understood as a metamorphosis (see Haug & Haug 2013, 2015 for the challenges of the term). The possibly more obvious later one is the transition from the last larval stage (erichthus) into the juvenile, involving a significant change of life style: while the erichthus larva is a pelagic/planktic predator, the juvenile becomes a benthic predator.

There is also an earlier significant change in life style. The antizoea lacks raptorial appendages and hence is a non-raptorial pelagic/planctic larva. Therefore, the transition to the erichthus also account for at least a smaller metamorphosis.

Specimen A obviously is right in the middle of this transition. While it strongly resembles specimen B in most aspects, there are already some characters that indicate its transition into the erichthus: 1) The antennula should be "uniramous" in the antizoea (e.g. Ahyong et al. 2014), but is already possessing two flagella in specimen A (Fig. 3B, C). 2) Pleopods should be still absent or at least non-functional (e.g. Ahyong et al. 2014); yet at least the anterior pleopods appear quite functional already (Fig. 5). 3) Most important: while maxillipeds 1 and 3-5 are still biramous and appear to be still functional as swimming appendages, maxilliped 2 clearly already shows the subdivision and coarse organisation of the later raptorial appendage (Fig. 4).

With this, specimen A represents an intermetamorphic form (term from Haug & Haug 2016). Such a stage seems to have been not reported for stomatopods in the literature so far and provides us with an interesting correlation (further discussed below).

In comparison to the "normal" antizoea morphology as represented by specimen B, certain aspects of the developmental pattern can be recognised. Only maxilliped 2 is further developed, the other maxillipeds are still in antizoea-type morphology. This is in concordance with the fact that maxilliped 2 is the largest of the series in later stages. This size difference may be simply explained either by 1) a peramorphic pattern for maxilliped 2 (by acceleration and/or pre-displacement) or 2) a paedomorphic pattern for the other maxillipeds (post-displacement or neoteny). This again emphasises the importance of heterochrony in stomatopod evolution (Haug & Haug 2015).

It must currently remain unclear whether specimen A represents a normal, so far simply not recognised stage, or an unusual derivation from the norm. In either case it provides interesting information. In how far this morphology is a regularly appearing one under natural conditions can be only judged in future studies.

Morphology of the raptorial appendage of specimen A

The exopod is clearly visible on the large raptorial appendage of specimen A, while the remaining appendage already partly has attained the morphology of a functional sub-chelate ballistic claw of the later stages. With this we have indeed the identifier demanded by Schram (2007). The morphology of the attachment area of the exopod strictly outlines the exact position of the disto-lateral rim of the basipod. This clearly indicates that the basipod is not conjoined with the next distal element, nor with the coxa.

Consequences for the 'missing-element problem' of stomatopod raptorial appendages

The new finding in fact not fully resolves the problem. Yet, the observation indeed provides new aspects. We can now clearly exclude that there is a coxo-basis (as suggested by Ahyong pers. com. in Schram 2007; Fig. 10A) or a basi-ischium (as suggested by Gruner 1993; Fig. 10B).

We therefore know for sure that we have an endopod with only four elements. With this, either the most distal element (or another one?) is entirely missing or, more likely, two of the original five endopod elements have become conjoined. Although we have now the exopod as an important marker point, we still have to involve other data for clearly identifying how the endopod morphology was transformed in the course of evolution.

Possible interpretation of fossil forms in the light of the new findings

Most interpretations of possible conjoined states within the endopod seem to vote for a conjoined state of the original ischium and merus (Hothuis & Manning 1969; McLaughlin 1980; Schram 1986; Westheide & Rieger 2007; Fig. 10C). Yet, we should also consider that more distal elements could have become conjoined (Fig 10D-F). Additionally, this evolutionary novelty of only four endopod elements does not necessarily need to account for the ground pattern of Stomatopoda, but may have evolved within the lineage. In this respect the following should be considered:

Schram (2007) suggested that there is an evolutionary change of the main joint of the raptorial claw within the stomatopod lineage: In modern forms the jackknifing joint is between the elements three and four, counted from distally (usually addressed to as carpus and merus, e.g. Schram 2007). In forms that show an overall more plesiomorphic morphology (e.g. species of *Gorgonophonthes*; Fig. 11A) the jackknifing joint is in a different position; between the elements four and five counted from distally. Schram (2007) also noted that the presumed carpus (element three counted from distally) is closely associated with the propodus (element two counted from distally) in these forms.

In fossil mantis shrimps we often have the distal parts of the appendages preserved, while the more proximal ones are often concealed (see discussion in Haug J.T. et al. 2010). While we have indeed cases in which all joints can be observed (examples in Haug J.T. et al. 2010; Haug C. et al. 2015), especially Palaeozoic forms mainly preserved the distal parts. This makes a clear identification of the individual elements at least challenging.

Given these observations, we propose that it is most likely that early stomatopods, all of the "palaeostomatopods" and some of the "archaeostomatopods" of Schram (2007, 2008; see also Haug J.T. et al. 2010 for discussion of these terms) still possessed five endopod elements. The jackknifing joint in these forms is between the elements four and five counted from distally, hence between merus and ischium. Within the stomatopod lineage (most likely at the node of Unipeltata sensu lato; Haug J.T. et al. 2010), two of the original five endopod elements become conjoined. From comparison of the joints it seems most likely that these are the carpus and the propodus (elements two and three counted from distally; Fig. 11 B). This interpretation would not require an evolutionary change of the jackknifing joint and is therefore seen as the most parsimonious explanation of the available data. This interpretation should be further corroborated by a future re-investigation of the cruzial fossils.

Conclusion

Given the new observations on larval extant stomatopods we can suggest that:

– the stomatopod maxillipeds do have a "normal" coxa and basipod. The smaller number of elements must be due to a conjoined state of endopod elements.

– In the light of this finding it seems likely that modern forms have a carpo-propodus.

– The study also demonstrates that intermetamorphic forms can provide important information for the identification of corresponding structures and improving evolutionary reconstructions.

FIJI.

References

Ahyong, S. T., & Harling, C. (2000). The phylogeny of the stomatopod Crustacea. *Australian Journal of Zoology*, *48*(6), 607-642.

Ahyong, S. T., Haug, J. T. & Haug, C. 2014. Stomatopoda. In: Martin, J. W., Olesen, J. & Høeg, J. T. (eds.), Atlas of Crustacean Larvae, 185–189. The Johns Hopkins University Press, Baltimore.

Gohar, H. A. F., & Al-Kholy, A. A. (1957): The larval stages of three stomatopod Crustacea. Publications of the Marine Biological Station, Al-Ghardaqa, Red Sea, **9**: 85–130.

Greenwood, J.G., and B.G. Williams. 1984. Larval and early post-larval stages in the abbreviated development of *Heterosquilla tricarinata* (Claus, 1871) (Crustacea, Stomatopoda). Journal of Plankton Research 6: 615–635.

Gruner, H.-E., et al. (Hg.) (1993): Lehrbuch der speziellen Zoologie: Wirbellose Tiere. *Arthropoda* (ohne *Insecta*). G. Fischer. 1279 pp.

Hamano, T., Matsuura, S. (1987): Egg size, duration of incubation, and larval development of the Japanese mantis shrimp in the laboratory. Nippon Suisan Gakkaishi, 53(1), 23-39.

Haug, C., Haug, J. T. (2014): Defensive enrolment in mantis shrimp larvae (Malacostraca Stomatopoda). Contributions to Zoology, 83(3), p. 185-194.

Haug, C., Haug, J. T., Waloszek, D., Maas, A., Frattigiani, R. & Liebau, S. 2009. New methods to document fossils from lithographic limestones of southern Germany and Lebanon. Palaeontologia Electronica 12(3); 6T; 12p.

Haug, C., Sallam, W. S., Maas, A., Waloszek, D., Kutschera, V. & Haug, J. T. (2012): Tagmatization in Stomatopoda–reconsidering functional units of modern-day mantis shrimps (Verunipeltata, Hoplocarida) and implications for the interpretation of fossils. Frontiers in Zoology, 9(1), p. 1-14.

Haug, C., Shannon, K. R., Nyborg, T., and Vega, F. J. (2013): Isolated mantis shrimp dactyli from the Pliocene of North Carolina and their bearing on the history of Stomatopoda. Bolétin de La Sociedad Geológica Mexicana 65(2), 273–284.

Haug, C., Wiethase, J. H. & Haug, J. T. 2015. New records of Mesozoic mantis shrimp larvae and their implications on modern larval traits in stomatopods. Palaeodiversity 8, 121–133.

Haug, J. T., Haug, C. (2013): An unusual fossil larva, the ontogeny of achelatan lobsters, and the evolution of metamorphosis. Bulletin of Geosciences, 88, p. 195-206.

Haug, J. T. & Haug, C. 2015. "Crustacea": Comparative aspects of larval development. In: Wanninger, A. (ed.), Evolutionary Developmental Biology of Invertebrates 4: Ecdysozoa II: Crustacea. Springer, Wien, 1–37.

Haug, J. T., Haug, C. (2016): "Intermetamorphic" developmental stages in 150 million-year-old achelatan lobsters – The case of the species *tenera*. Arthropod Structure & Development, doi:10.1016/j.asd.2015.10.001

Haug, J. T., Haug, C., and Ehrlich, M. (2008): First fossil stomatopod larva (Arthropoda: Crustacea) and a new way of documenting Solnhofen fossils (Upper Jurassic, Southern Germany). Palaeodiversity *1*, 103–109.

Haug, J. T., Haug, C., Maas, A., Kutschera, V. & Waloszek, D (2010): Evolution of mantis shrimps (Stomatopoda, Malacostraca) in the light of new Mesozoic fossils. BMC evolutionary Biology, 10.

Haug, J. T., Haug, C., Kutschera, V., Mayer, G., Maas, A., Liebau, S., Castellani, C., Wolfram, U., Clarkson, E.N., and Waloszek, D. (2011): Autofluorescence imaging, an excellent tool for comparative morphology. Journal of Microscopy 244(3), 259– 272.

Haug, J. T., Briggs, D. E. G. & Haug, C. 2012. Morphology and function in the Cambrian Burgess Shale megacheiran arthropod *Leanchoilia superlata* and the application of a descriptive matrix. BMC Evolutionary Biology 12, art. 162.

Holthuis, L., Manning, R. (1969): Stomatopoda,. Treatise on Invertebrate Paleontology, Part R, Arthropoda, 4. R535-R552.

Hörnig, M. K., Haug C., Herd K. J., Haug J. T. (2014): New insights into dictyopteran early development: small- est Palaeozoic roachoid nymph found so far. *Palaeodiversity*, 7: 159-165.

Manning, R. B., Provenzano Jr, A. J. (1963): Studies on Development of Stomatopod CrustaceaI. Early Larval Stages of *Gonodactylus Oerstedii Hansen*. Bulletin of Marine Science, 13(3), 467-487.

McLaughlin, P. A. (1980): In: McLaughlin, P. A. Comparative morphology of recent Crustacea, pp. 177. San Francisco: WH Freeman.

Morgan, S.G. and J.G. Goy 1987. Reproduction and larval development of the mantis shrimp *Gonodactylus bredini* (Crustacea: Stomatopoda) maintained in the laboratory. Journal of Crustacean Biology 7: 595–618.

Morgan, S. G., & Provenzano Jr, A. J. (1979): Development of pelagic larvae and postlarva of *Squilla empusa* (Crustacea, Stomatopoda) with an assessment of larval characters within the Squillidae. – Fishery Bulletin, **77** (1): 61–90.

Provenzano Jr, A. J., & Manning, R. B. (1978): Studies on development of stomatopod crustacea II. The later larval stages of *Gonodactylus oerstedii* Hansen reared in the laboratory. – Bulletin of Marine Science, **28** (2): 297–315.

Pyne, R. R. (1972): Larval development and behaviour of the mantis shrimp, *Squilla armata* Milne Edwards (Crustacea: Stomatopoda). – Journal of the Royal Society of New Zealand, **2** (2): 121–146.

Schram, F. R. (1986). Crustacea. Oxford University Press, New York 1-606 .

Schram, F. R. (2007): Paleozoic proto-mantis shrimp revisited. Journal of Paleontology, 81(5), p. 895-916.

Schram, F. R. (2008): An adjustment to the higher taxonomy of the fossil Stomatopoda. In: Crustaceana, 81(6), p. 751-754.

Walossek, D. (1993). The upper Cambrian Rehbachiella and the phylogeny of Branchiopoda and Crustacea. *Lethaia*, *26*(4), 318-318.

Walossek, D.,Müller, K. J. (1998): Cambrian 'Orsten'-type arthropods and the phylogeny of Crustacea. Journal: Arthropod relationships. In: Fortey, R.R. & Thomas, R. (eds.): Arthropod relationships, Systematics Association Special Volume 55, 139-153. Chapman & Hall, London.Springer Netherlands.

Waloszek, D. (2003): "The'Orsten'window-a three-dimensionally preserved Upper Cambrian meiofauna and its contribution to our understanding of the evolution of Arthropoda." Paleontological Research 7(1), p. 71-88.Westheide, W., & Rieger, R. (2007): Spezielle Zoologie, Vol. 1: Einzeller und wirbellose Tiere. Spektrum Akademischer Verlag, München. 982pp.

Wiethase, J., Haug, J.T. & Haug, C. (in review). Identifying heterochronic events in mantis shrimp evolution: first attempts. International Journal of Evolutionary Biology.

Wolff, C, Scholtz, G. (2008): The clonal composition of biramous and uniramous arthropod limbs. Proceedings of the Royal Society of London B: Biological Sciences, 275(1638), p. 1023-1028.

Figure captions

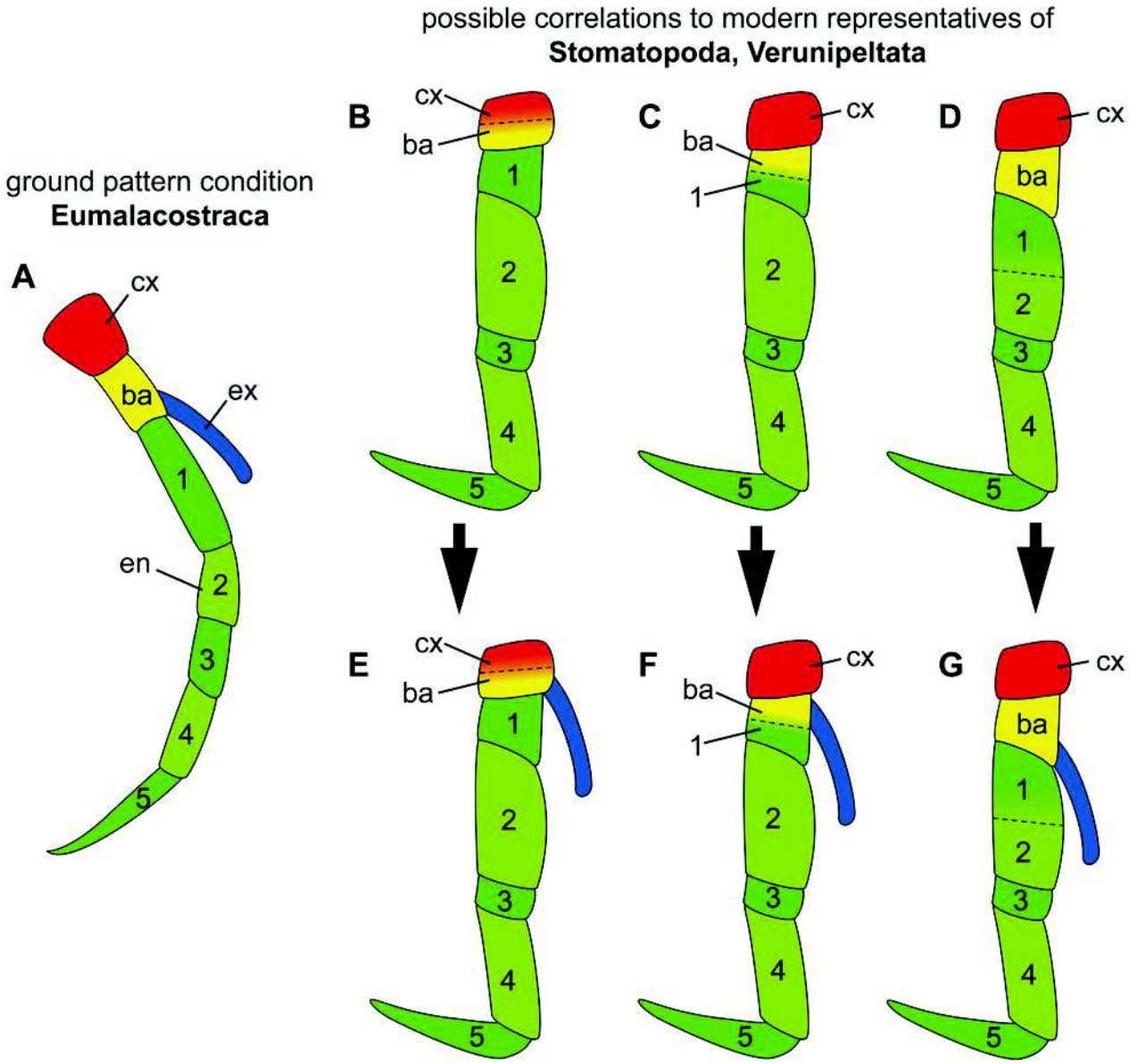

Figure 1: Schematic representations of thoracic appendages in the ground pattern of Eumalacostraca and within Stomatopoda. A. Simplified eumalacostracan thoracopod with 7 elements (coxa, basipod and 5 endopod elements) along main axis. B-D. Suggested correlations in modern mantis shrimps. B. With a coxo-basis. C. With a basi-ischium. D. With an ischio-merus. E-G. To be expected insertion of the exopod. E. Disto-laterally on element 1 for coxo-basis. F. Proximo-laterally on element 2 for basi-ischium. G. Disto-laterally on element 2 for ischio-merus. Abbreviations: ba = basipod; cx = coxa; en = endopod; ex = exopod; 1 = endopod element 1, ischium; 2 = endopod element 2, merus; 3 = endopod element 3, carpus; 4 = endopod element 4, propodus; 5 = endopod element 5 = dactylus. Colour scheme following Walossek (1993).

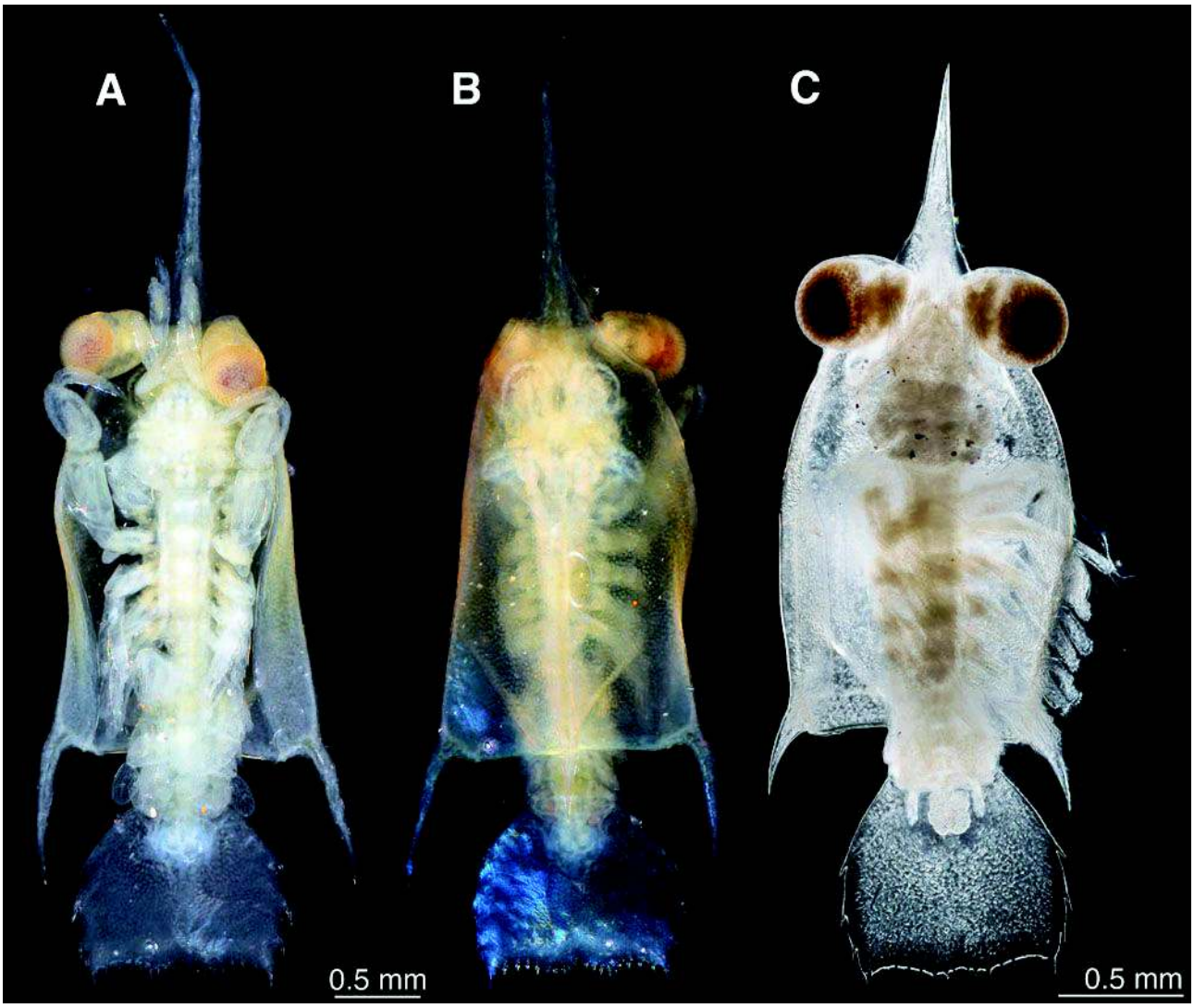

Figure 2: Overview images of two stomatopod larvae under white light. A, B. Composite-macrophotographic images (under cross-polarized light) of specimen A (ZMUC 3723_V_E). A. Ventral view. B. Dorsal view. C. Composite image, transmitted light; specimen B (ZMUC 3567_II_A); ventral view.

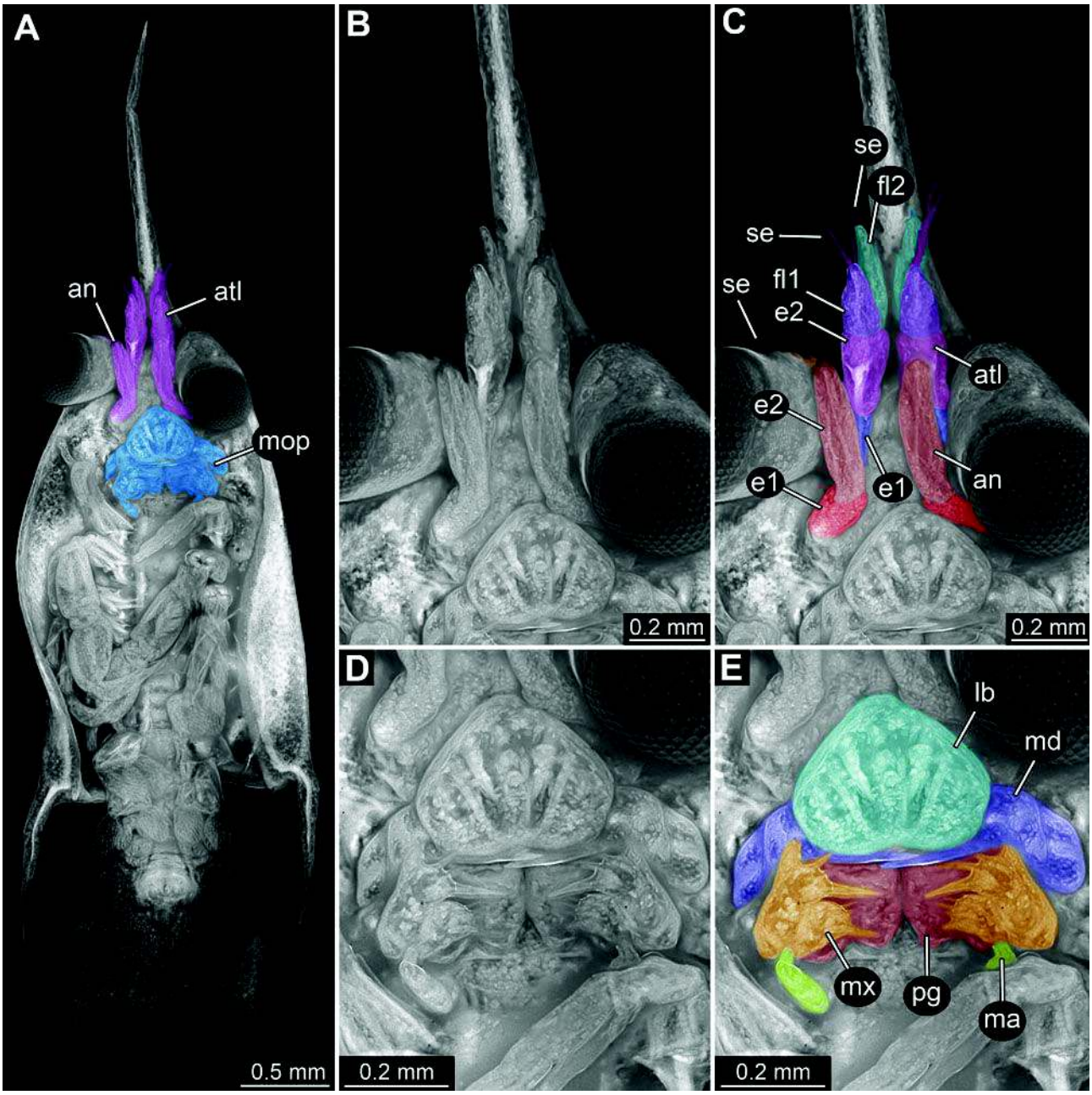

Figure 3: Details of sensorial and feeding apparatus of specimen A. All images composite autofluorescence images. A. Colour-marked overview image in ventral view; antennula and antenna (pink) and mouthparts (blue). B. Close-up on antennula and antenna. C. Colour-marked version of B; with antennula (in violet, blue, cyan) and antenna (in red). D. Close-up on mouth parts. E. Colour-marked version of D; labrum (cyan), mandible (violet-blue), paragnaths (red), maxillula (orange) and maxilla (green). Abbreviations: an = antenna, atl = antennula; e1,2 = element 1, 2; fl1, 2 = flagellum 1, 2; lb = labrum; ma = maxilla; md = mandible; mop = mouth parts; mx = maxillula; pg = paragnaths; se = seta.

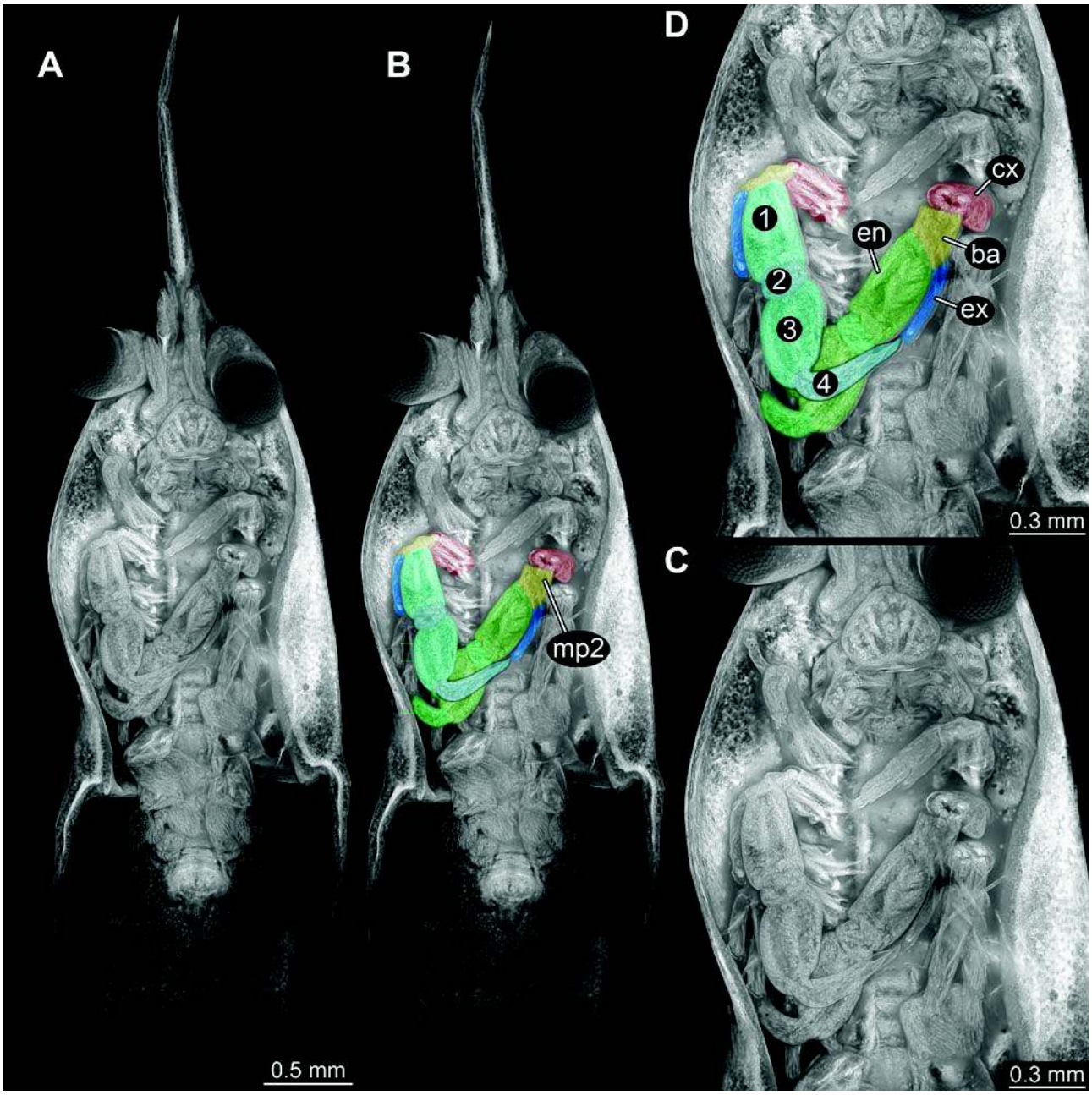

Figure 4. Details of maxilliped 2 of specimen A. All images composite autofluorescence images. A. Ventral view of entire specimen. B. Colour-marked version of A, emphasising the second maxilliped. C. Close-up on second maxilliped. D. Colour-marked version of C. Abbreviations: ba = basipod; cx = coxa; en = endopod; ex = exopod; 1-4 = observable elements of the endopod. Colour scheme following Walossek (1993).

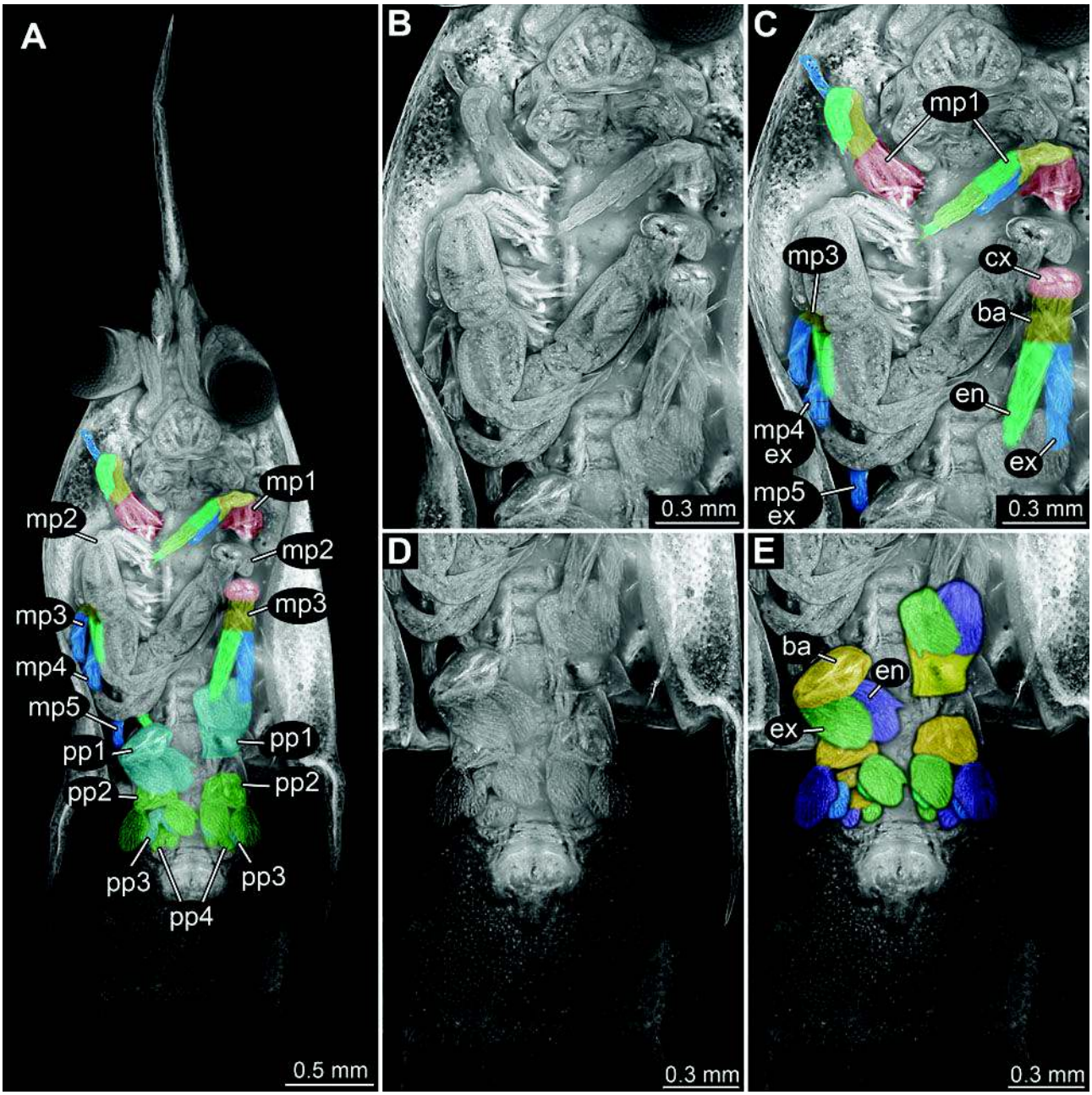

Figure 5. Details of trunk appendages of specimen A. Overview image with colour-marked maxillipeds (with the exception of maxilliped 2 which is shown in Fig. 4) and pleopods. B. Close-up on maxillipeds. C. Colour-marked version of B. D. Close-up on pleopods. E. Colour-marked version of D. Abbreviations: ba = basipod; cx = coxa; en = endopod; ex = exopod; mp1-5 = maxillipeds 1-5; pp1-4 = pleopods 1-4. Colour scheme following Walossek (1993).

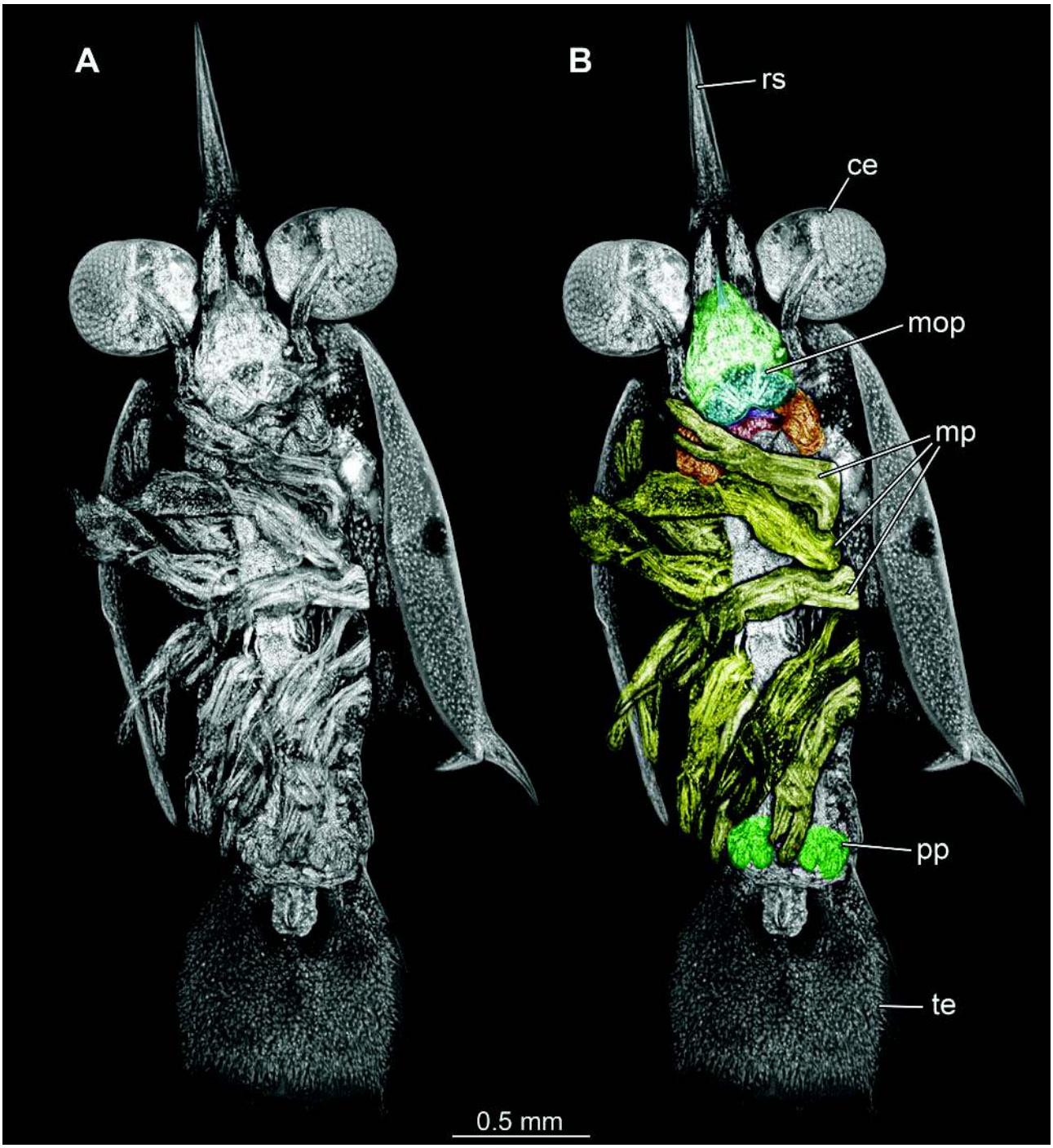

Figure 6. Overview image of specimen B; cLSM images. A. Ventral view. B. Colour-marked version of A: mouthparts (green, blue, orange, red), maxillipeds (yellow), pleopods (green). Abbreviations: ce = compound eye; mop = mouth parts; mp = maxilliped; pp = pleopod; rs = rostral spine; te = telson.

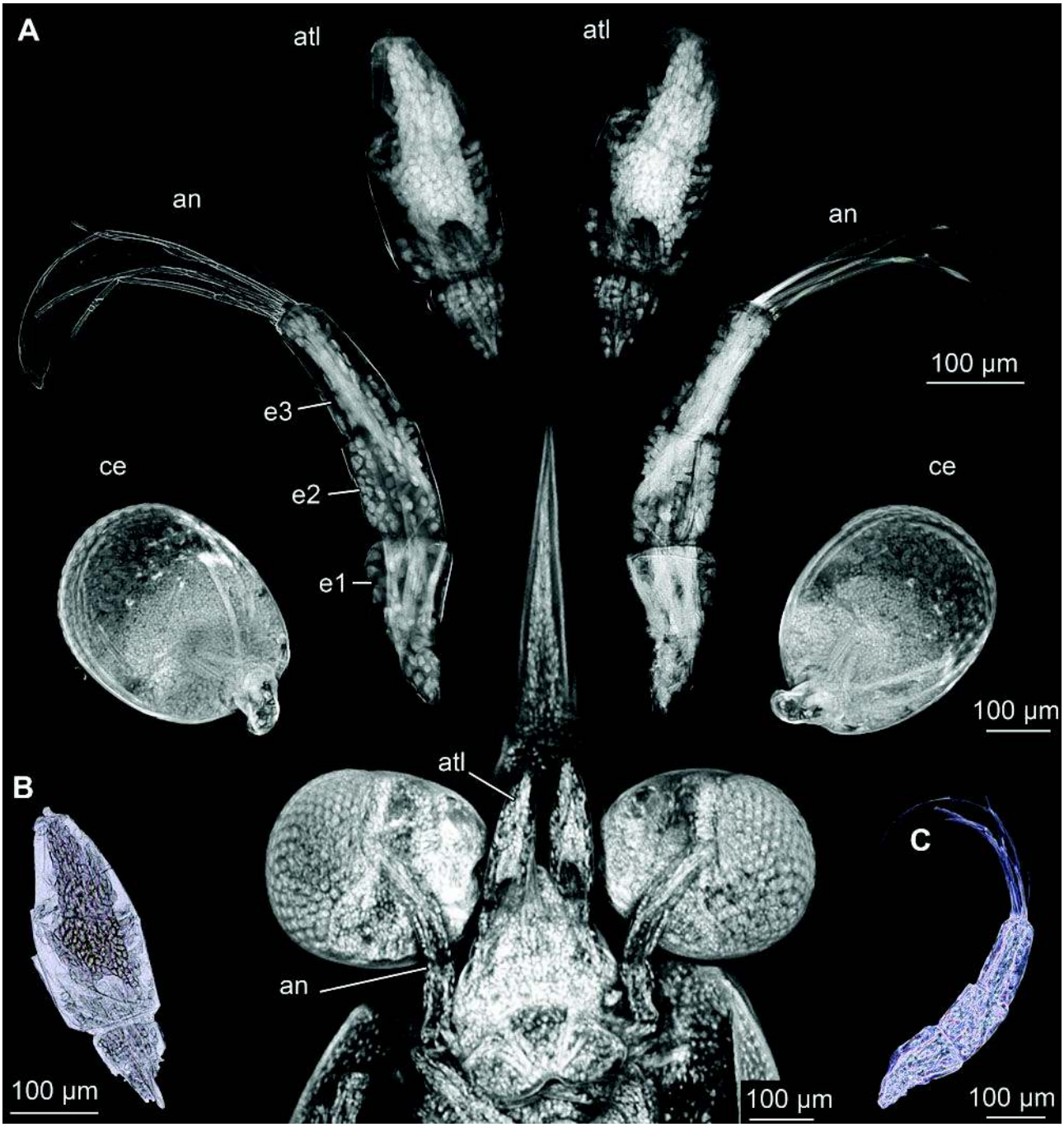

Figure 7. Close-up on sensorial structures of specimen B. A. Details of isolated antennula, antennae and compound eyes (all auto-fluorescence images) and in original position cLSM image. B. Isolated antennula, transmitted light bright field. C. Isolated antennae, transmitted light phase contrast. Abbreviations: an = antenna; atl = antennula; ce = compound eye; e1-3 = elements 1-3.

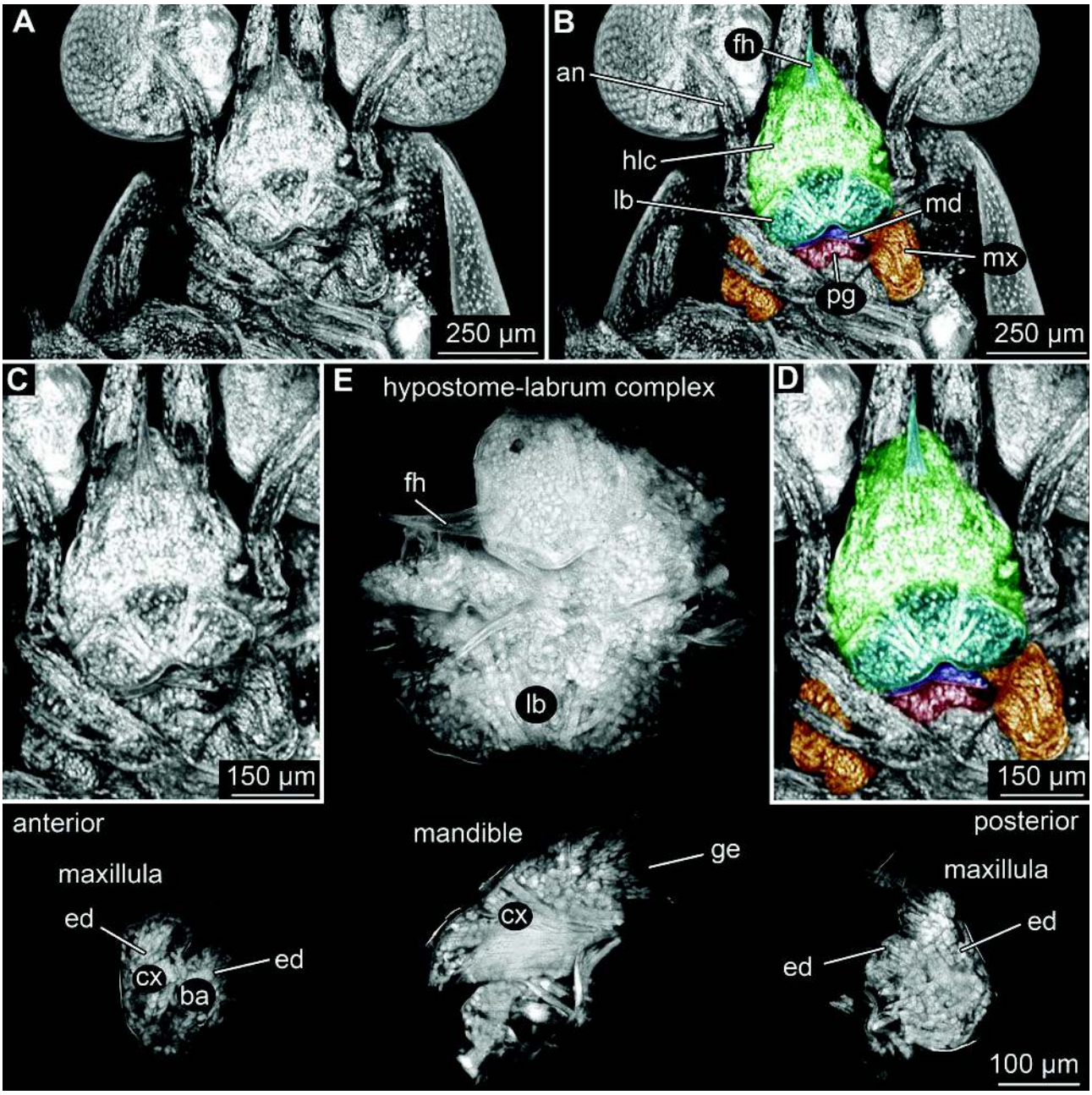

Figure 8. Close-up on feeding apparatus of specimen B. A-D cLSM images; E epi-fluorescence images. A. Anterior region in ventral view. B. Colour-marked version of A with frontal horn (cyan), hypostome-labrum complex (green), labrum (cyan), mandible (violet), maxillula (orange), paragnaths (red). C. Close-up on mouthparts. D. Colour-marked version of C. E. Isolated mouthparts, hypostome-labrum complex, mandible and maxillula from both sides (damaged during re-positioning). Abbreviations: an = antenna; ba = basipod; cx = coxa; ed = endite; fh = frontal horn; ge = gnathal edge; hlc = hypostom-labrum complex; lb = labrum; md = mandible; mx = maxillula; pg = paragnaths;

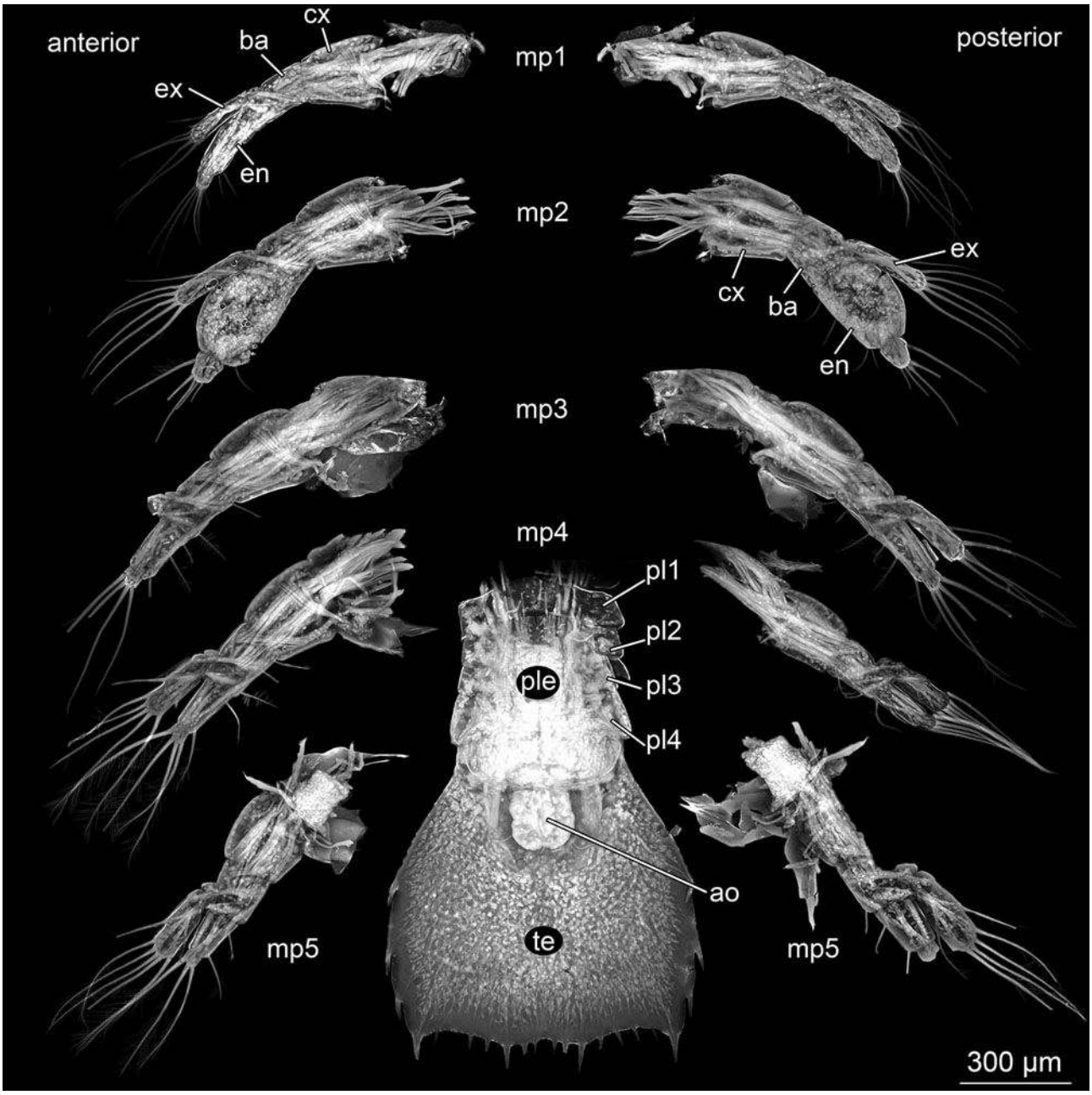

Figure 9. Auto-fluorescence images of maxillipeds and pleon of specimen B. Left: anterior views of maxilliped. Right: posterior views of maxillipeds. Lower middle: ventral view of pleon. Abbreviations: ao = anal opening; ba = basipod; cx = coxa; en = endopod; ex = exopod; mp1-5 = maxillipeds 1-5; pl1-4 = pleonal segments 1-4; ple = pleon; te = telson.

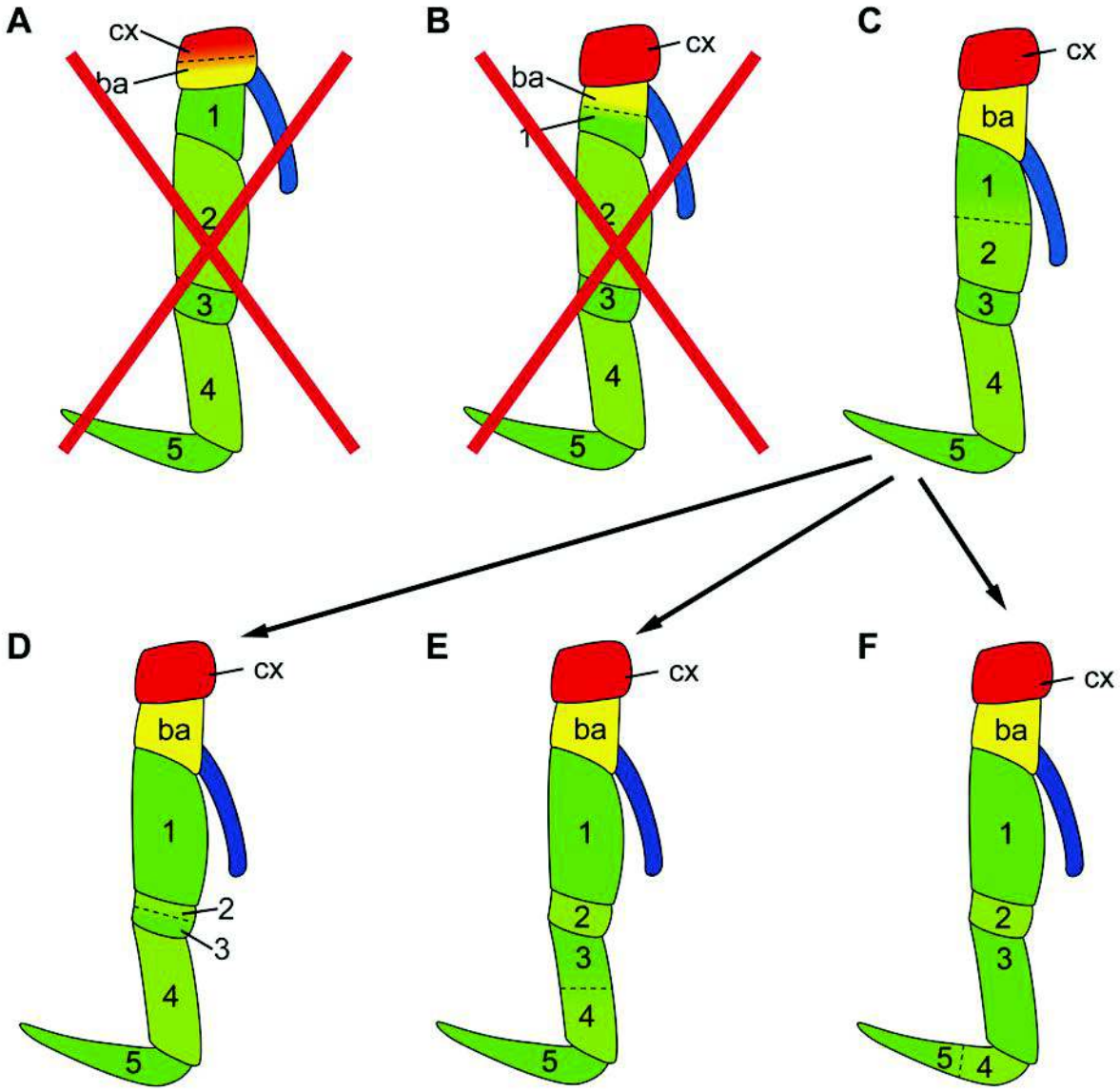

Figure 10. Schematic representations of interpretations of thoracic appendages within Stomatopoda. A-C suggested correlations in modern mantis shrimps. A. With a coxo-basis => rejected. B. With a basi-ischium => rejected. C. With an ischio-merus => possible, but in fact not the only possible one. D-F. Alternative interpretations also compatible with the observed exopod position in specimen A. D. With a mero-carpus. E. With a carpo-propodus. F. With a propodo-dactylus. Abbreviations: ba = basipod; cx = coxa; en = endopod; ex = exopod; 1 = endopod element 1, ischium; 2 = endopod element 2, merus; 3 = endopod element 3, carpus; 4 = endopod element 4, propodus; 5 = endopod element 5 = dactylus. Colour scheme following Walossek (1993).

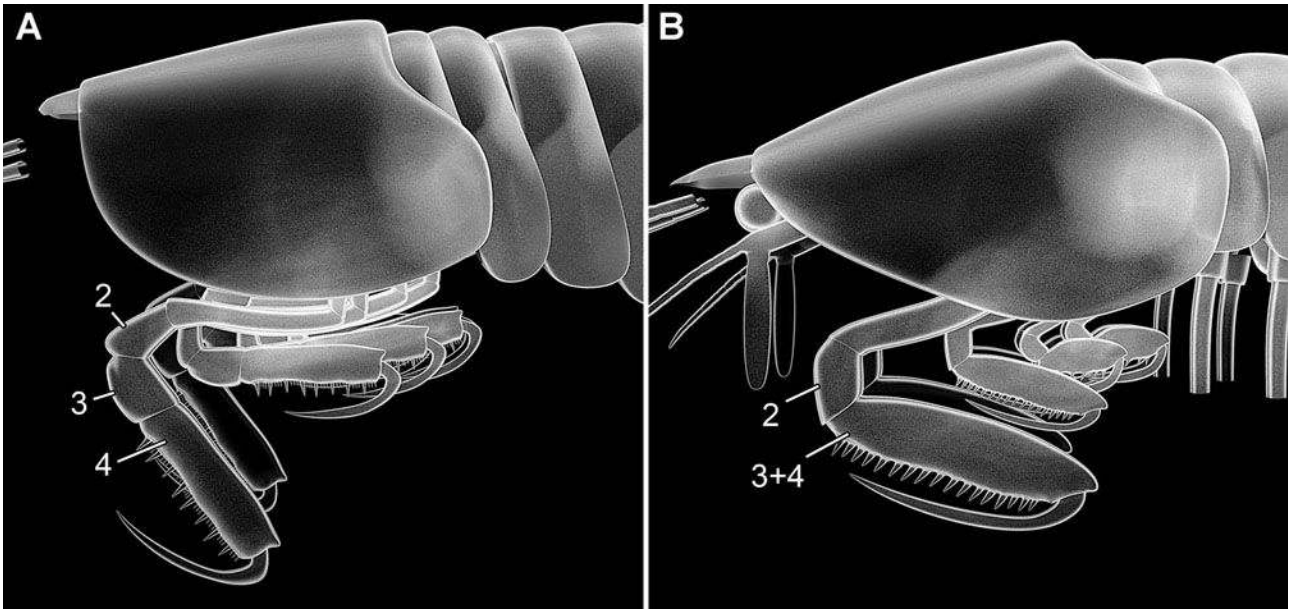

Figure 11: Simplified 3D models of the Palaeozoic mantis shrimps *Gorgonophontes* sp. and *Tyrannophontes* sp. (see Haug J.T. et al. 2010) and suggested elemental correlation of raptorial appendages. A. *Gorgonophontes* sp. with separate carpus and propodus. B. *Tyrannophontes* sp. with conjoined carpus and propodus. Abbreviations: 2-4 = endopod elements 2-4 (merus, carpus, propodus).